# Modelling of RC moment resisting frames with precast-prestressed flooring system

B.H.H. Peng, R.P. Dhakal, R.C. Fenwick & A.J. Carr

*Department of Civil Engineering, University of Canterbury, Christchurch.*

D.K. Bull

*Holmes Consulting Group Ltd., Christchurch.*

**2009 NZSEE Conference**

**ABSTRACT:** In this paper, the seismic performance of reinforced concrete moment resisting frames coupled with a floor containing precast-prestressed units is examined. Mechanisms associated with the beam strength enhancement arising from plastic hinges and floor interactions are described. A computational model is set up to predict the response of a 3D frame containing precast-prestressed floor units with cast-in-situ concrete topping. This model contains newly developed plastic hinge elements which account for flexural, shear and elongation response of plastic hinges in beams subjected to inelastic rotation and varying axial load levels. To allow for floor interaction with the beam plastic hinges, the model uses axial strut-and-tie elements to represent the linking slab between the longitudinal beams and the first precast unit. Analysis using this model shows good agreement with the experimental results indicating that the model can be used to analyse the seismic performance of RC frames containing precast-prestressed flooring systems.

## 1 INTRODUCTION

Recent experimental studies at Canterbury and Auckland universities on the seismic performance of reinforced concrete (RC) moment resisting frames coupled with precast-prestressed flooring systems have shown that the presence of prestressed floor units increases the strength of the beams more than that specified in the New Zealand code. This level of strength enhancement has raised concern as it may shift the designed ductile beam sway mechanism to an undesirable column sway mechanism.

The level of strength enhancement varies with different structural arrangements. The mechanisms associated with the strength enhancement in previous tests have been described by Fenwick et al. (2006; 2005). One of the strength enhancement mechanisms arises from prestressed floor units spanning pass an intermediate column, and thus providing restraining force against elongation of the interior plastic hinges. The other strength enhancement mechanism arises from prestressed floor units, supported on transverse beams, confining the major cracks to the weak section at the supports. This provided additional tension force to the negative flexural strength of plastic hinges.

While these tests gave some insight into the level of strength enhancement expected to occur in frames with prestressed flooring units, the results cannot readily be used to develop satisfactory design rules due to wide range of structural arrangements used in practice. Repetitive experimental studies on this topic would be complex, time and resource consuming. Therefore, to provide a more feasible alternative, numerical simulation has to be explored.

To analytically simulate the strength enhancement of beams in moment resisting frames coupled with prestressed floor units, the computational model must contain plastic hinge elements that can predict elongation response of plastic hinges as well as floor slab elements that allow for interactions with the elongating plastic hinges. This paper describes a computational model set up in RUAUMOKO3D (Carr 2008) to simulate a 3D sub-assembly test unit of a 2 bay moment frame coupled with a floor slab containing prestressed floor units (Peng et al. 2008).

## 2 EXPERIMENTAL SET-UP

The test unit consisted of a one storey, two bay moment-resisting frame with transverse beams connected into each column and with a floor slab containing prestressed units as shown in Figure 1. The floor consists of 100mm deep precast-prestressed ribs supported on transverse beams with 45mm thick cast-in-situ concrete topping. Grade 300, 10mm deformed bars were placed in the concrete topping at 210mm centers in both directions. These were lapped to 10mm starter bars along the perimeter beams. The floor was connected to a 175mm thick end slab to represent the stiff continuation of floor diaphragm in the rest of the building.

Columns in the moment frames were supported on two way linear bearings to allow movement in the horizontal plane. The exterior transverse beams were supported on steel columns with one way linear bearing allowing floor movement parallel to the moment resisting frame. The interior transverse beam was supported on steel column with ball bearings that allow floor movement in the horizontal plane. Loading was displacement controlled; quasi-static cyclic loading was applied to the top and bottom of each column in the plane of the moment resisting frame through six hydraulic rams. Within each loading increment, the displacements at the top and bottom of each column were corrected iteratively to ensure that the columns remained parallel to each other and that beam elongation was not externally restrained and no axial load was induced in the longitudinal beams by the hydraulic rams.

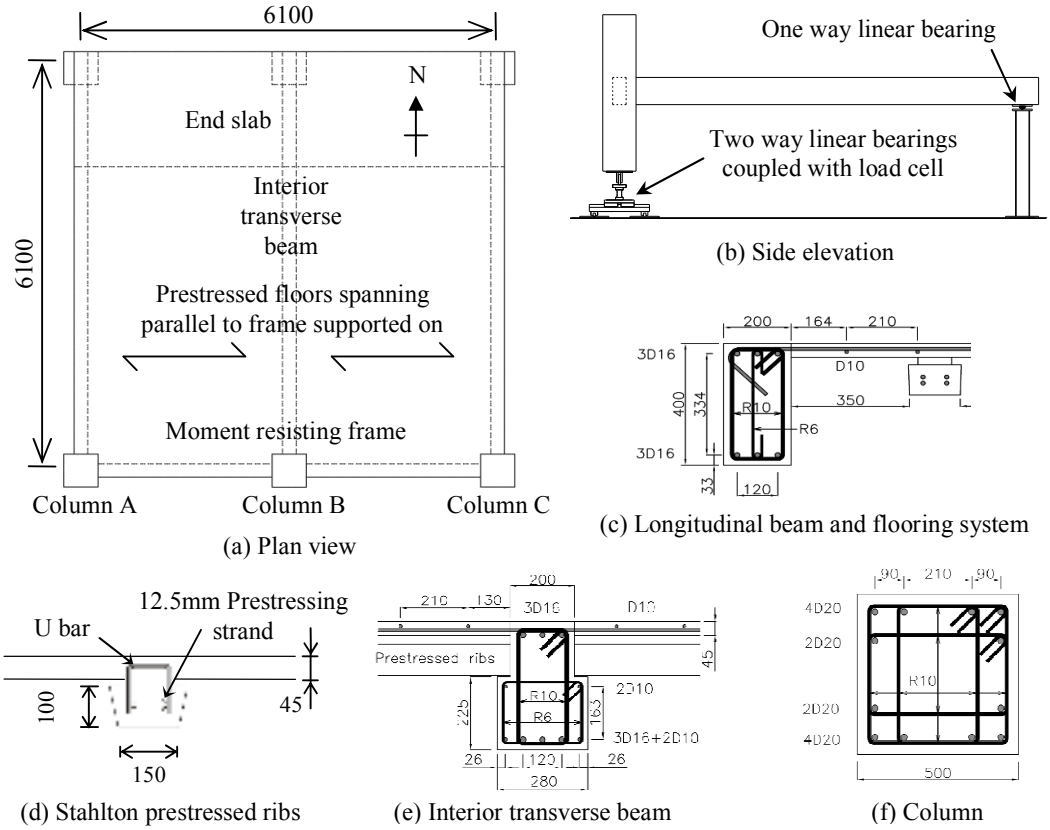


Figure 1. Experimental set-up and key section details

## 3 3D COMPUTATIONAL MODELLING

### 3.1 Model set-up

The overall layout of the analytical model is illustrated in Figure 2. The model contains several layers of nodes and elements located at the centre line of each member section. The columns, beam column

joints, transverse beams, elastic portion of longitudinal beam, prestressed ribs and end slab are modelled using elastic Giberson beam element. The plastic hinges in the longitudinal beams are modelled using elongating plastic hinge element developed by the authors (Peng et al. 2007). Axial truss members are inserted over the "linking slab" (floor slab between the first rib unit and the longitudinal beam) and along the interface between floor topping and transverse beams where large non-linearity is expected. The rest of the floor topping is modelled using elastic quadrilateral shell elements which take into account plane stress and plate bending. The details of these members are described later in the paper. The boundary conditions are the same as in the experiment.

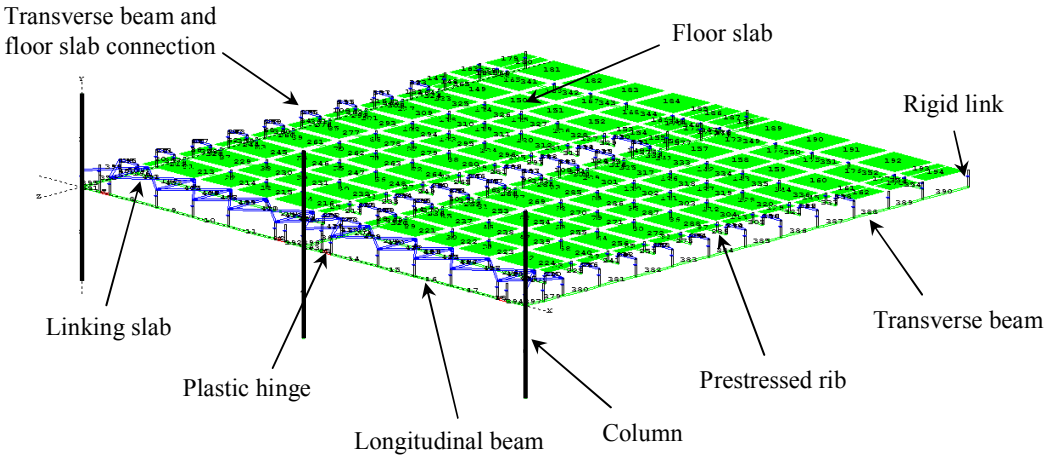


Figure 2. Layout of the 3D analytical model

## 3.2 **Member properties**

### 3.2.1 *Plastic hinge element*

Figure 3(a) shows a schematic diagram of the plastic hinge element. The development and verification of the plastic hinge element are described in details elsewhere (Peng et al. 2007). The element consists of a series of longitudinal and diagonal axial springs connected between rigid links at two ends. The longitudinal concrete and steel springs are used to represent the flexural response of the plastic hinge, and the diagonal springs are used to represent the diagonal compression struts in the web as shown in Figure 3(b), which also provide shear resistance. The plastic hinge element is controlled by two key parameters: the length of the plastic hinge element, $L_P$ and the effective length of the steel spring, $L_{yield}$.

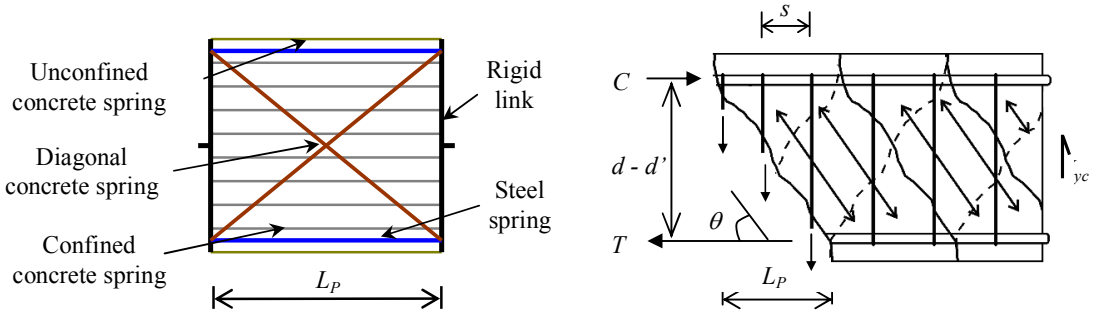


(a) Analytical plastic hinge element (b) Diagonal crack patterns in RC beams

Figure 3. Plastic hinge element

The length of the plastic hinge element, $L_P$, represents the inclination of the diagonal compression struts in the plastic hinge. It is hypothesized that the diagonal cracks will form in an angle such that it crosses enough stirrups to resist the shear force in the web. Consequently, $L_P$ can be expressed as a function of the stirrup spacing as shown in Equation 1 where $V_{yc}$ is the shear force corresponding to

the flexural strength of the beam, $M_{yc}$, $s$ is the stirrup spacing, and $A_v$, $f_{vy}$ are the area and yield strength of the shear reinforcement. From the experimental results, the shear force in the beam at formation of plastic hinges (at 1% drift) is 87kN and the corresponding $L_P$ is 105mm.

$$L_P = \frac{V_{yc} s}{A_v f_{vy}} \tag{1}$$

The effective length of steel spring, $L_{steel}$, is taken as the length over which the reinforcement yields and is given by Equation 2, where $M/V$ is the moment to shear ratio, $M_{max}$ is the maximum moment sustained in the beam, $L_t$ is the length of tension shift and $L_e$ is the length of yield penetration into the support. The average maximum strength measured in the experiment was 1.2 times the averaged yield strength of the beam. The length of tension shift is calculated assuming no axial force existed in the member. This resulted in an effective steel spring length, $L_{steel}$, of 458mm.

$$L_{steel} = \frac{M}{V}\frac{M_{max} - M_{yc}}{M_{max}} + L_t + L_e \tag{2}$$

The compressive strength of the concrete confined within the stirrups is calculated based on equations proposed by Mander et al. (1988) and is equal to $1.2f'_c$. The compressive strength of the diagonal springs is set as $0.34f'_c$ recommended by To et al. (2001) and the tensile strength of the diagonals is set close to zero.

### 3.2.2 *Elastic beams, columns, beam-columns, prestressed ribs and end slab*

The elastic member properties are based on cracked concrete sections with the effective moment of inertia being taken as $0.4I_{gross}$. The elastic modulus is taken as Young's modulus of concrete, $E_c$, and the shear modulus of member, $G$, is taken as $0.4E_c$. These values are consistent with the New Zealand Standard, NZS3101:2006. The torsional second moment of area, $J$, is taken as $bh(b^2+h^2)/12$ where $b$ and $h$ are the width and depth of the section. Shear deformation is neglected in the elastic member.

The nominal torsional capacity of the transverse beams, $T_n$, is based on the torsional capacity of reinforcement specified in NZS3101:2006 and is given in Equation 3, where $A_o$ is the gross area enclosed by shear flow path, $A_t$ is the area of one leg of the closed stirrup, $f_{yt}$ and $f_y$ are the yield strength of the stirrup and longitudinal bars respectively, $s$ is the spacing of the stirrup, $A_l$ is the area of the longitudinal bars and $p_o$ is the length of perimeter of section measured between centres of reinforcing bars in corners of the member. A bilinear factor of 0.02 is used for post torsional yielding strength.

$$T_n = 2A_o\sqrt{\frac{A_t f_{yt}}{s}\frac{A_l f_y}{p_o}} \tag{3}$$

### 3.2.3 *Linking slab*

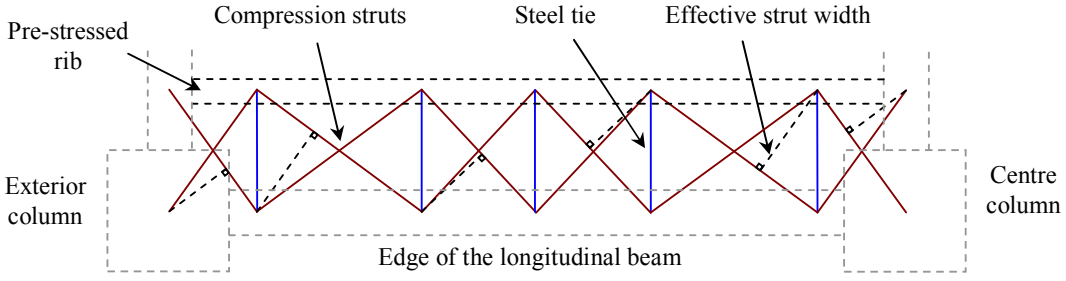


Figure 4. Schematic diagram showing the effective width of diagonal struts

The linking slab is modelled using strut-and-tie analogy. The diagonal struts are modelled using concrete springs and the transverse ties are modelled using steel springs. These axial springs are

located at the mid-height of the floor slab. The length of the concrete spring is taken as the length of the element. The length of the steel spring is taken as the clear width of the linking slab plus half of the development length into the floor slab plus a portion of the development length into the longitudinal beam. The development length is calculated based on NZS3101:2006. The area of the concrete strut is taken as the effective strut width, as illustrated in Figure 4, multiplied by the thickness of the slab. The tensile strength of the diagonal struts is assigned a very small value.

#### 3.2.4 *Floor topping and transverse beam interface*

It is assumed that the moment capacity of the interface between floor topping and transverse beams is negligible due to wide cracks developing as a result of plastic hinge elongation. Therefore, the interface is modelled by a series of axial steel and concrete springs located at the mid-height of floor topping along the transverse beams. The length of the steel spring is taken as half of the development length into the floor slab plus a portion of the development length into the transverse beam.

## 4 ANALYTICAL PREDICTION AND COMPARISONS WITH EXPERIMENTAL RESULTS

### 4.1 Force-displacement response

The analytical and experimental force-displacement relationships for the overall frame and each individual column are shown in Figure 5. It can be seen that the analysis predicts both the loading and unloading stiffness together with the yield force and the peak force accurately. Note that this model has not been calibrated to fit the experimental results. The elongating plastic hinge elements as well as the truss-like floor elements are based on stress-train relationships of concrete and reinforcing bars which do not require calibration. Pinching was underestimated in the analysis. This is due to bond degradation and slipping of reinforcing bars in the beam-column joints not being considered in the analysis. It can be seen that pinching is predicted more accurately in the exterior columns compared to the interior column. This is because the bars were anchored more effectively in the exterior plastic hinges and therefore the corresponding slip and the difference in pinching is less dramatic.

Yielding of the longitudinal reinforcement in the exterior plastic hinges occurred close to 1% drift. Maximum lateral force of 333kN was reached at 3% drift. The provisions in NZS 3101:2006 for calculating the over-strength of T-beams with a flange on one side are based on empirical results (Lau 2007; Lindsay 2004; MacPherson 2005). The calculated effective flange width for the theoretical flexural strength of the exterior and interior plastic hinge is 360mm. The corresponding negative and positive flexural strength of the beam is 85.3kNm and 72.6kNm. This gives a total column shear force of 198kN as shown in Figure 5(a).

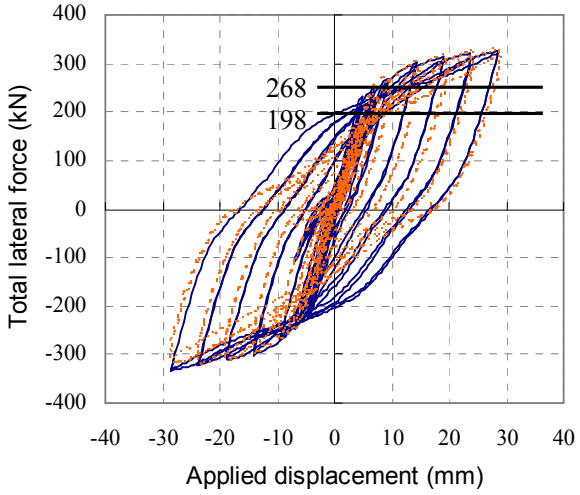


(a) Overall force-displacement comparison

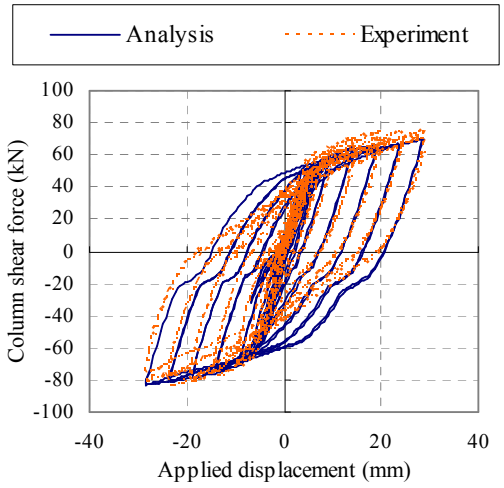


(b) Force-displacement Column A

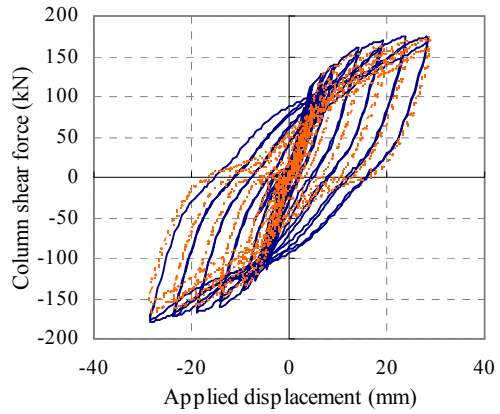


(c) Force-displacement Column B

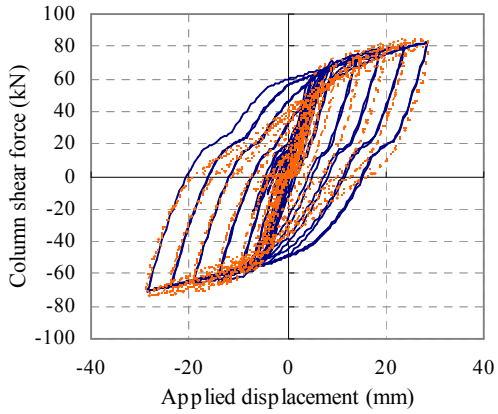


(d) Force-displacement Column C

Figure 5. Analytical and experimental force-displacement comparisons

According to NZS3101:2006, the effective flange width for calculating the negative over-strength of the exterior and interior plastic hinges is 900mm and 1200mm respectively in the test. In addition, the code specifies that the stress of the slab reinforcement be taken as $1.1\phi_o f_y$ where $\phi_o$ is the over-strength factor equal to 1.25 for Grade 300 steel. Note that the over-strength value in the code assumes a 15% increase in yield stress based on the statistical upper 95 percentile value plus a 10% increase for strain-hardening. In the experiment, the actual material yield stress was measured and hence an over-strength value of 1.1 was used for calculating the over-strength of the beams. The negative over-strength of the exterior and interior plastic hinges is 125.8kNm and 142.5kNm respectively and the positive over-strength of the plastic hinge is 79.2kNm. The corresponding total column shear force is equal to 268kN as shown in Figure 5(a). It can be seen that the code specified column strength is significantly lower than the experimentally measured and analytically predicted values.

### 4.2 **Beam elongation**

The analytical and experimental elongation histories for the exterior and interior plastic hinges are shown in Figure 6. The analysis predicts elongation of the interior and exterior plastic hinges accurately up to 2.5% drift. Analytical elongation is smaller in the negative drifts than in the positive drifts as shown in Figure 6(a) because reinforcement in the floor slab induced axial compression force to the plastic hinge in the negative drift cycles. It is under investigation why elongations at positive and negative drifts are similar in the experiment.

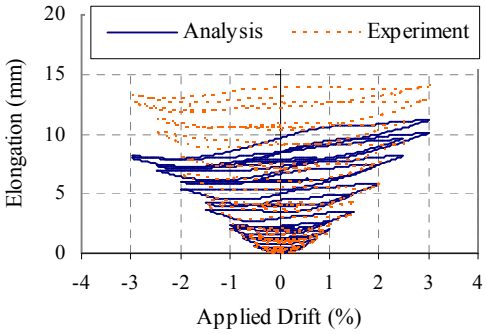


(a) West bay exterior plastic hinge

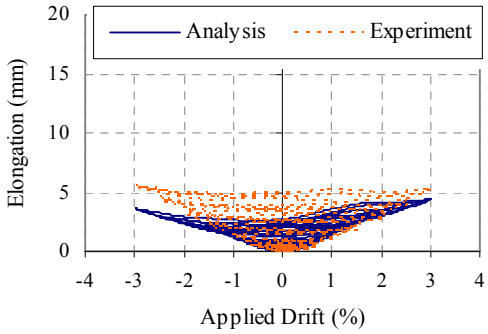


(b) East bay interior plastic hinge

Figure 6. Analytical and experimental elongation comparisons

### 4.3 **Cracks width between the transverse beams and floor topping**

The prediction of crack widths along the transverse beam to floor topping interface is important as it

controls the extent of reinforcement participation in the floor slab and therefore the strength enhancement in the beams. Comparisons between the analytical and experimental crack widths along this interface at 3% drift are summarised in Table 1. It can be seen that the analysis predicts the crack widths with reasonable accuracy. As can be seen in the table, crack widths near the exterior plastic hinge are underestimated in the analysis. This can be attributed to the elongation in the exterior plastic hinge being underestimated in the analysis at larger drift cycles.

**Table 1. Cracks width comparisons along the transverse beams and floor slab interface at 3% drift**

| Distance from the column face (mm) | Crack width behind exterior plastic hinge (mm) | | Crack width behind interior plastic hinge (mm) | |
|---|---|---|---|---|
| | Experiment | Analysis | Experiment | Analysis |
| 275 | 6.0 | 4.5 | 3.7 | 3.0 |
| 775 | 1.1 | 0.2 | 2.2 | 1.9 |
| 1275 | 0.2 | 0 | 1.1 | 1.3 |
| 1775 | 0.2 | 0 | 0.7 | 0.8 |
| 2275 | 0.1 | 0 | 0.4 | 0.5 |

## 5 STRENGTH ENHANCEMENT MECHANISMS

Enhancement in the column shear force, observed in the experiment and analysis, arises due to two main mechanisms:

1. Torsional resistance of the transverse beams increases the column shear force in both positive and negative drift directions. It is difficult to separate out the torsional resistance of transverse beams from the experimental results. At the end of the test, the longitudinal beams were removed and cyclic displacements were applied to the columns to measure the torsional resistance of the transverse beams. The storey shear force obtained from the test at 3% drift was 25kN. As the transverse beams had been extensively cracked prior to the torsional test, the torsional resistance of the transverse beams could have been much higher than that measured in this test. The nominal torsional strength of the exterior and interior transverse beams calculated based on NZS3101:2006 is 35.5kNm and 40.5kNm respectively, which corresponds to a storey shear force of 59kN.
2. Reinforcement in the slab participates in the negative flexural strength of the beam. From the cracks width measured at the weak sections along the transverse beam to floor topping interface, the number of bars which yielded in the slab can be interpreted and the corresponding tension force estimated. The crack widths corresponding to yielding of reinforcing bars in the experiment is approximately 0.4mm. The interpreted effective flange width next to the interior and exterior plastic hinges at 3% drift is 1200mm and 2200mm respectively, which give over-strength moments of 131kNm and 176kNm.

**Table 2. Over-strength enhancement from different mechanisms**

| | Averaged column shear force (kN) | | | Total shear force (kN) |
|---|---|---|---|---|
| | Column *A* | Column *B* | Column *C* | |
| Transverse beam torsion | 18.6 | 21.3 | 18.6 | 58.5 |
| Floor slab participation | 54.4 | 157.9 | 79.9 | 292.2 |
| TOTAL | 73.0 | 179.2 | 98.5 | 350.7 |
| 1st cycle at +3.0 % | 76.4 | 171.6 | 85.6 | 333.6 |

The column shear force enhancement arises from these two mechanisms is quantified in Table 2 based on experimental observations. It can be seen that the combined forces from the torsional resistance of transverse beams and floor slab participation agree reasonably well with the experimental results. The comparisons also show that the torsional resistance of the transverse beam contribute to about 17% of the total column shear force. This is currently ignored in the code. However, the torsional resistance would greatly reduce if plastic hinges formed in the transverse beams.

## 6 CONCLUSIONS

The experimental and analytical results in this paper highlight the importance of floor participation and torsional resistance of transverse beams in the post yielding behaviour of RC moment resisting frames. The results show that the current New Zealand Concrete Structures Standard underestimates the flexural strength of beams where prestressed flooring units span parallel to the frame supported on transverse beams. The computational model developed in this paper predicts the strength of the frame and the interaction between beams and floor under inelastic cyclic actions with reasonable accuracy. A case study will be carried out at the end of this research to examine the strength enhancement associated with real building frames with multiple bays.

## REFERENCES


Carr, A. J. (2008). "RUAUMOKO3D - Inelastic Dynamic Analysis." Department of Civil Engineering, University of Canterbury, Christchurch, New Zealand.

Fenwick, R. C., Bull, D. K., MacPherson, C., and Lindsay, R. "The Influence of Diaphragms on Strength of Beams." New Zealand Society for Earthquake Engineering Conference 2006.

Fenwick, R. C., Davidson, B. J., and Lau, D. B. N. "Interaction between Ductile RC Perimeter Frames and Floor Slabs Containing Precast Units." New Zealand Society for Earthquake Engineering Conference 2005, Page 23-35.

Lau, D. B. N. (2007). "Influence of precast prestressed flooring on the seismic performance of reinforced concrete perimeter frame buildings." Report Number 653, Dept. of Civil and Environmental Engineering, University of Auckland, Auckland, New Zealand.

Lindsay, R. (2004). "Experiments on the Seismic Performance of Hollow-core Floor Systems in Precast Concrete Buildings," Master of Engineering Thesis, Department of Civil Engineering, University of Canterbury, Christchurch, New Zealand.

MacPherson, C. (2005). "Seismic Performance and Forensic Analysis of a Precast Concrete Hollow-core Floor Super-assemblage," Master of Engineering Thesis, Department of Civil Engineering, University of Canterbury, Christchurch, New Zealand.

Mander, J. B., Priestley, M. J. N., and Park, R. (1988). "THEORETICAL STRESS-STRAIN MODEL FOR CONFINED CONCRETE." Journal of Structural Engineering, 114(8), 1804-1826.

Peng, B. H. H., Dhakal, R., Fenwick, R., and Bull, D. "Experimental study on the seismic performance of reinforced concrete moment resisting frames with precast-prestressed floor units." New Zealand Society for Earthquake Engineering Conference 2008, Wairakei, NZ.

Peng, B. H. H., Dhakal, R., Fenwick, R., Carr, A., and Bull, D. "Analytical Model on Beam Elongation within the Reinforced Concrete Plastic Hinges." New Zealand Society for Earthquake Engineering Conference 2007, Palmerston North, NZ.

Standards New Zealand. (2006). Concrete Structures Standard: NZS3101:2006, Standards New Zealand, Wellington.

To, N. H. T., Ingham, J. M., and Sritharan, S. (2001). "Monotonic non-linear analysis of reinforced concrete knee joints using strut-and-tie computer models." Bulletin of the New Zealand Society for Earthquake Engineering, 34(3), 169-190.